The dipole photon strength of uranium isotopes from TAC measurements at n_TOF

Standa Valenta
for n_TOF collaboration

July 10, 2024

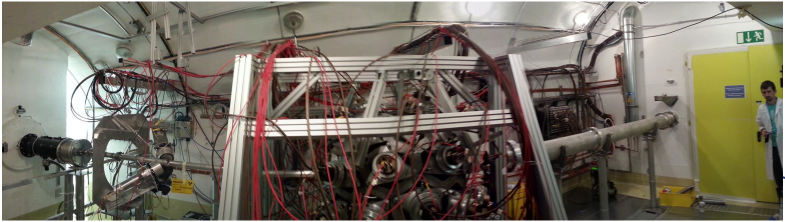

The dipole photon strength of uranium isotopes from TAC measurements at n_TOF

PHYSICAL REVIEW C **105**, 024618 (2022)

Constraints on the dipole photon strength for the odd uranium isotopes

J. Moreno-Soto,[1,*] S. Valenta,[2,†] E. Berthoumieux,[1] A. Chebboubi,[3] M. Diakaki,[3] W. Dridi,[4] E. Dupont,[1] F. Gunsing,[1,‡] M. Krtička,[2] O. Litaize,[3] O. Serot,[3] O. Aberle,[5] V. Alcayne,[6] S. Amaducci,[7] J. Andrzejewski,[8] L. Audouin,[9] V. Bécares,[6] V. Babiano-Suarez,[10] M. Bacak,[5,11,1] M. Barbagallo,[5,12] Th. Benedikt,[13] S. Bennett,[14] J. Billowes,[14] D. Bosnar,[15] A. Brown,[16] M. Busso,[17,18] M. Caamaño,[19] L. Caballero-Ontanaya,[10] F. Calviño,[20] M. Calviani,[5] D. Cano-Ott,[6] A. Casanovas,[20] F. Cerutti,[5] E. Chiaveri,[5,14] N. Colonna,[12] G. Cortés,[20] M. A. Cortés-Giraldo,[21] L. Cosentino,[7] S. Cristallo,[17,22] L. A. Damone,[12,23] P. J. Davies,[14] M. Dietz,[24] C. Domingo-Pardo,[10] R. Dressler,[25] Q. Ducasse,[26] I. Durán,[19] Z. Eleme,[27] B. Fernández-Domínguez,[19] A. Ferrari,[5] P. Finocchiaro,[7] V. Furman,[28] K. Göbel,[13] A. Gawlik-Ramięga,[8] S. Gilardoni,[5] I. F. Gonçalves,[29] E. González-Romero,[6] C. Guerrero,[21] S. Heinitz,[25] J. Heyse,[30] D. G. Jenkins,[16] A. Junghans,[31] F. Käppeler,[32,§] Y. Kadi,[5] A. Kimura,[33] I. Knapová,[2] M. Kokkoris,[34] Y. Kopatch,[28] D. Kurtulgil,[13] I. Ladarescu,[10] C. Lampoudis,[35] C. Lederer-Woods,[24] S. J. Lonsdale,[24] D. Macina,[5] A. Manna,[36,37] T. Martínez,[6] A. Masi,[5] C. Massimi,[36,37] P. Mastinu,[38] M. Mastromarco,[5] E. A. Maugeri,[25] A. Mazzone,[12,39] E. Mendoza,[6] A. Mengoni,[40] V. Michalopoulou,[5,34] P. M. Milazzo,[41] F. Mingrone,[5] A. Musumarra,[7,42] A. Negret,[43] R. Nolte,[26] F. Ogállar,[44] A. Oprea,[43] N. Patronis,[27] A. Pavlik,[45] J. Perkowski,[8] L. Piersanti,[17,22] C. Petrone,[43] E. Pirovano,[26] I. Porras,[44] J. Praena,[44] J. M. Quesada,[21] D. Ramos-Doval,[9] T. Rauscher,[46,47] R. Reifarth,[13] D. Rochman,[25] M. Sabaté-Gilarte,[21,5] A. Saxena,[48] P. Schillebeeckx,[30] D. Schumann,[25] A. Sekhar,[14] A. G. Smith,[14] N. V. Sosnin,[14] P. Sprung,[25] A. Stamatopoulos,[34] G. Tagliente,[12] J. L. Tain,[10] A. Tarifeño-Saldivia,[20] L. Tassan-Got,[5,34,9] P. Torres-Sánchez,[44] A. Tsinganis,[5] J. Ulrich,[25] S. Urlass,[31,5] G. Vannini,[36,37]

neutron_Time Of Flight facility

neutron_Time Of Flight facility

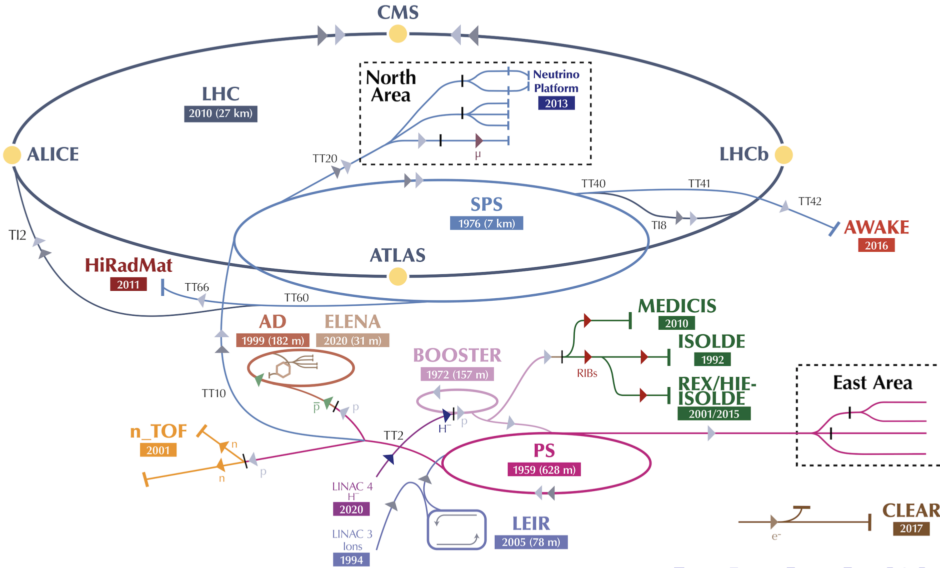

What is neutron time of flight?

Google

neutron time of flight

Prihlásiť sa

Všetko · Obrázky · Videá · Nákupy · Správy · Viac · Nástroje

Približne 6 720 000 výsledkov (0,46 sekundy)

The Neutron Time Of Flight (n-TOF) facility is a neutron spectrometer at CERN. It consists of a pulsed source, a flight path of 200 m length, and a detector systems. Neutron energies are deduced from the time of flight between source and detector; hence the name of the facility.

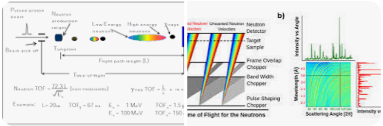

wikipedia.org
https://en.wikipedia.org › wiki › Neutron_Time_Of_Flight

Neutron Time Of Flight - Wikipedia

Vybrané úryvky • Spätná väzba

Podobné dopyty

- How fast is a neutron?
- What is the relation between the neutron wavelength and the time of flight over a particular distance?
- What is the temperature of thermal neutron?

Spätná väzba

Neutron Time Of Flight

Preložené z angličtiny - Zariadenie Neutron Time Of Flight je neutrónový spektrometer v CERN-e. Pozostáva z impulzného zdroja, dráhy letu s dĺžkou 200 m a systému detektorov. Energie neutrónov sú odvodené z času letu medzi zdrojom a detektorom; odtiaľ názov zariadenia. Wikipédia (angličtina)

What is neutron time of flight?

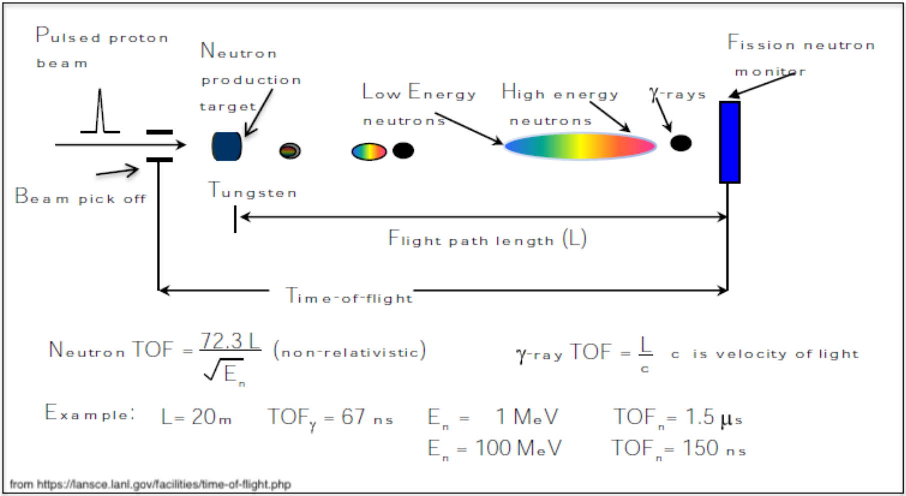

neutron_Time Of Flight facility

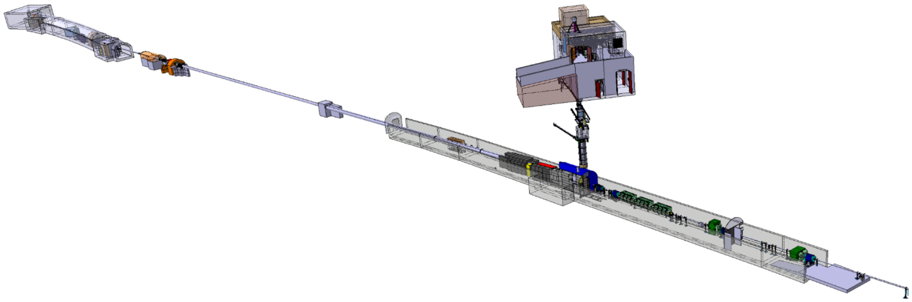

neutron_Time Of Flight facility

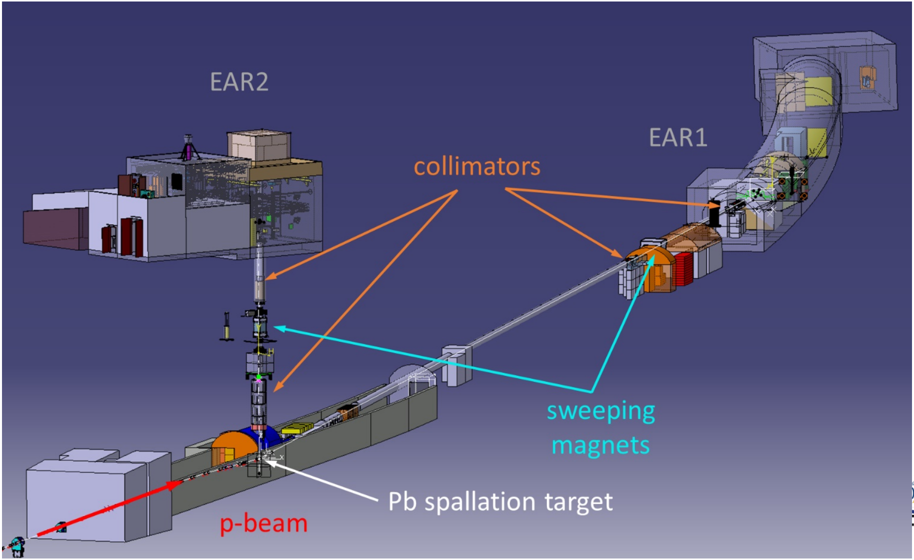

Experimental ARea 1

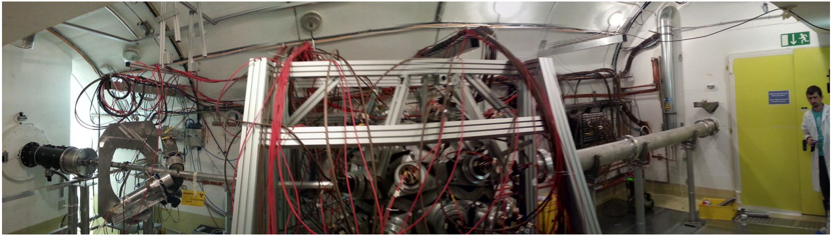

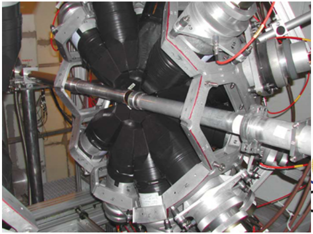

Experimental conditions & samples

	^{234}U	^{236}U	^{238}U
Mass (mg)	32.7	338	6125
Areal density (10^{-4} atoms/b)	1.07	10.9	9.56
Canning	Ti	Al	Al
$S_n^{\text{compound}} \approx Q$ (MeV)	5.297	5.126	4.806
Resolution @ 0.9 MeV (%)	14.5	16.5	16.5
Absorber	^{6}Li-salt	B-PE	B-PE

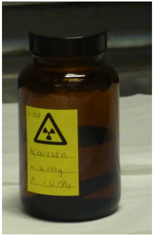

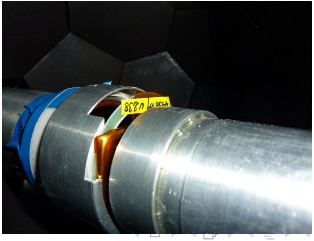

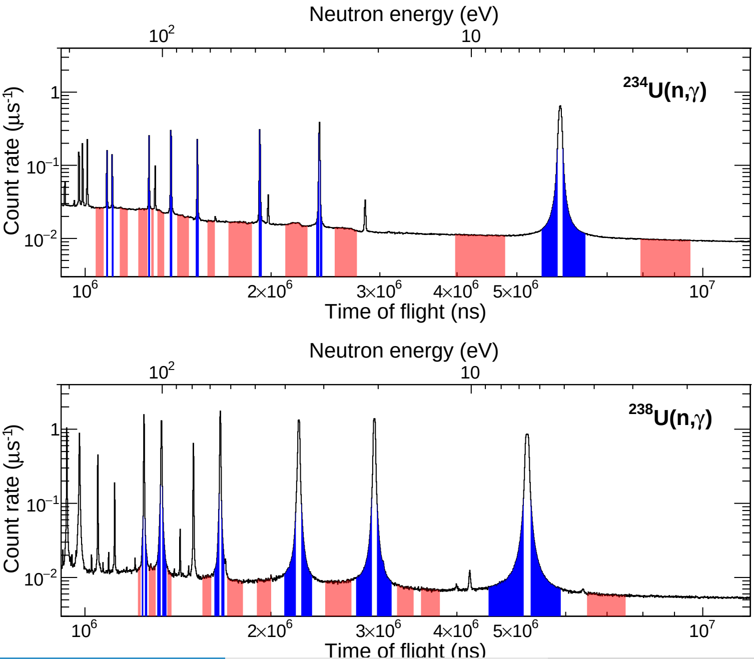
Neutron energy (eV)
10^2
10
Count rate (μs^-1)
1
10^-1
10^-2
234U(n,γ)
10^6
2×10^6
3×10^6
4×10^6
5×10^6
10^7
Time of flight (ns)
Neutron energy (eV)
10^2
10
Count rate (μs^-1)
1
10^-1
10^-2
238U(n,γ)
10^6
2×10^6
3×10^6
4×10^6
5×10^6
10^7
Time of flight (ns)

Spectra of energy sums for strong isolated resonances

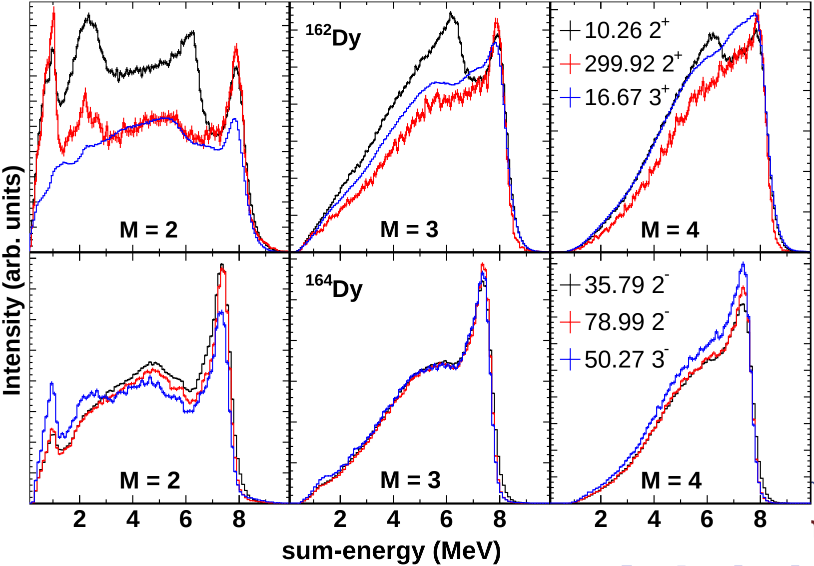

Spectra of energy sums for strong isolated resonances

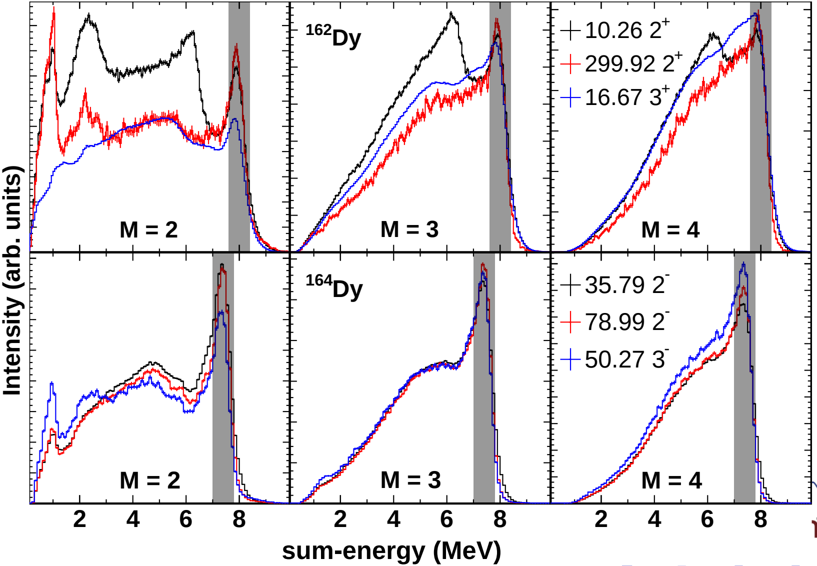

The energies forming the cascades ev-by-ev

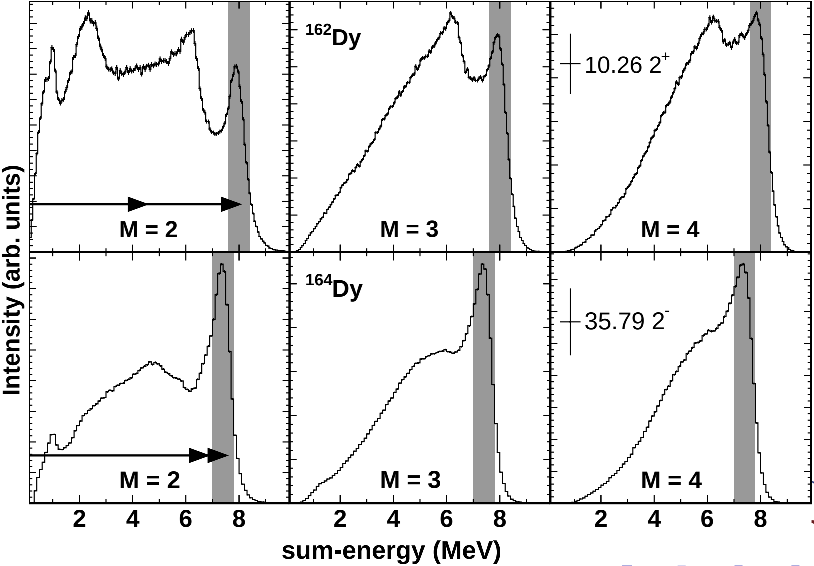

Experimental multi-step γ cascades (MSC) spectra

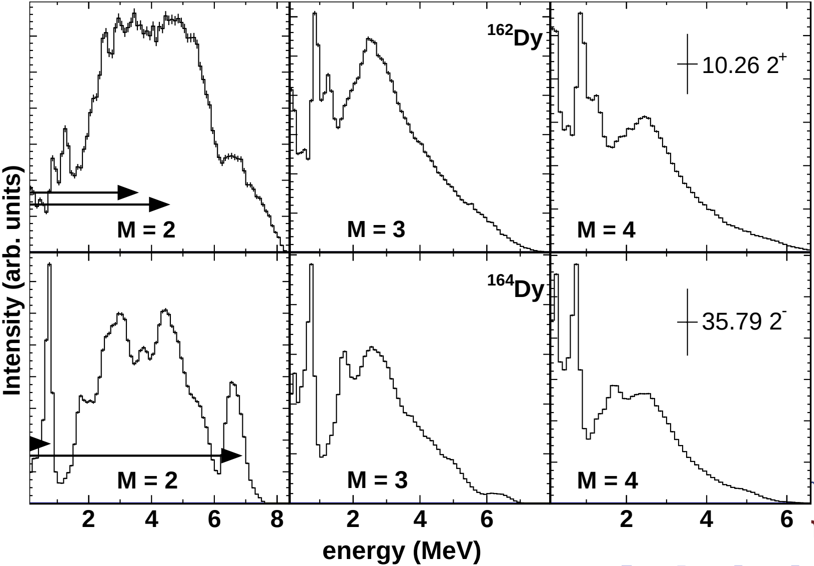

Experimental MSC spectra

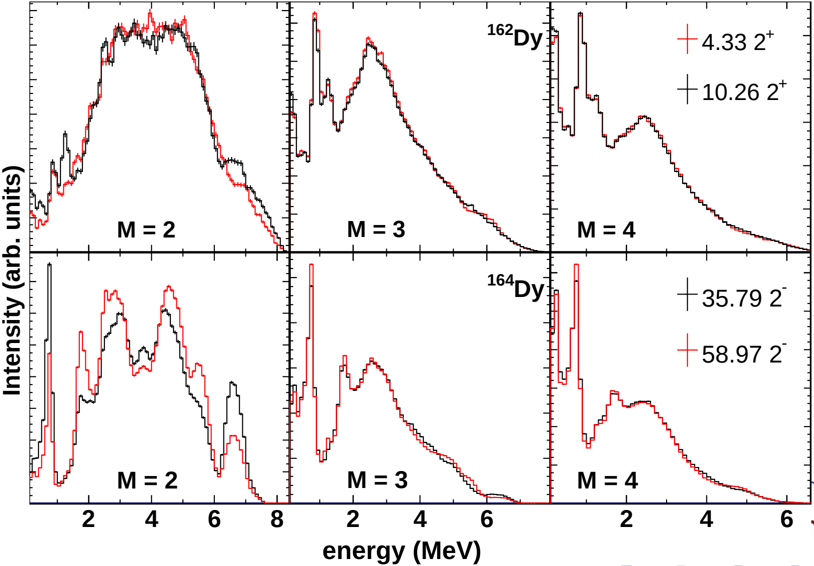

Experimental MSC spectra

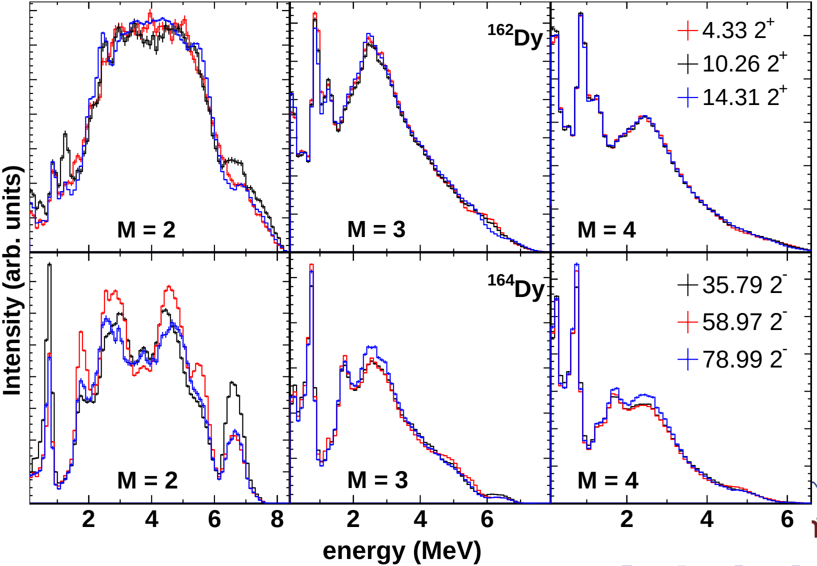

Experimental MSC spectra

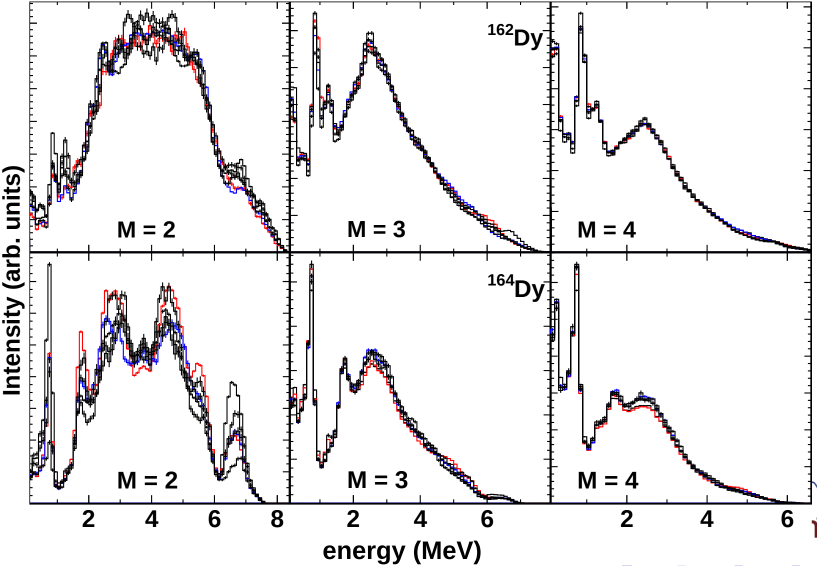

Experimental MSC spectra

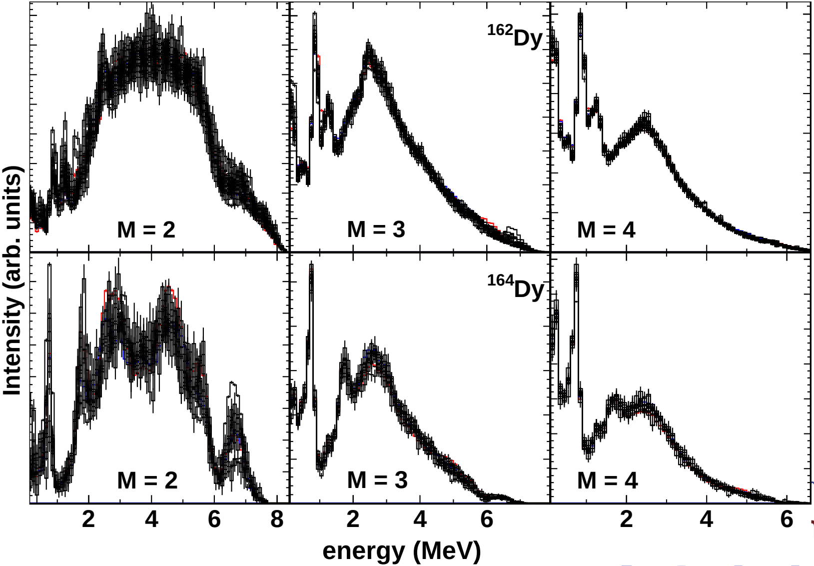

Average experimental MSC spectra

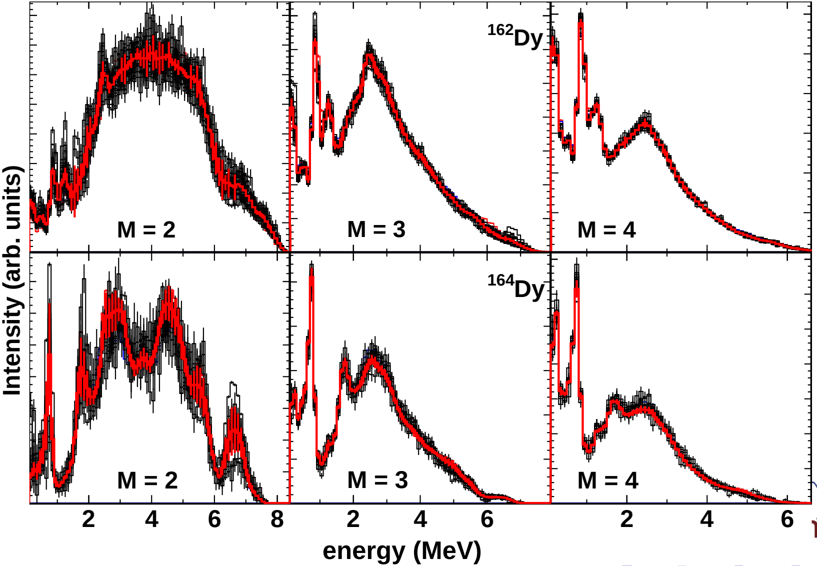

Average experimental MSC spectra

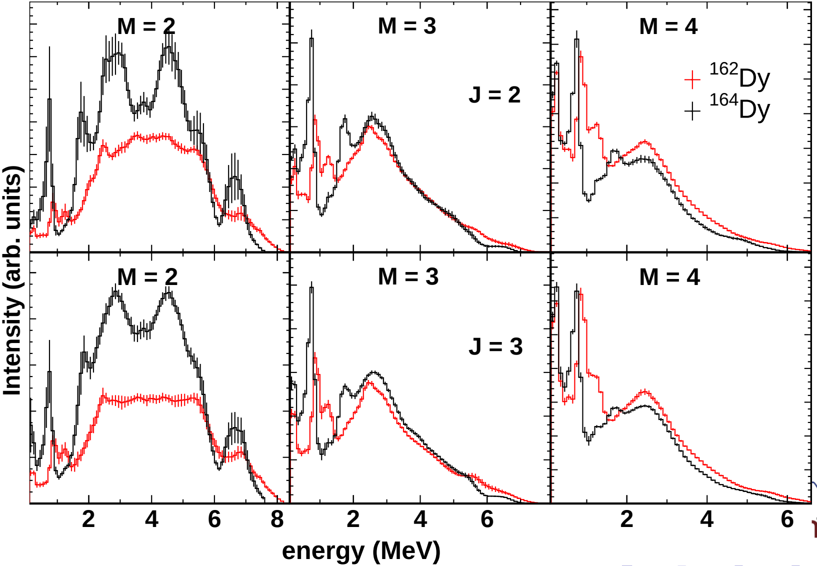

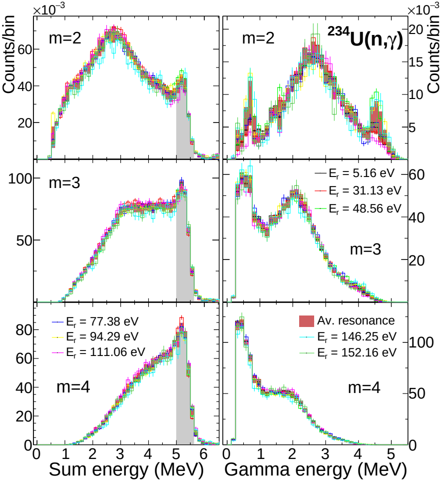
×10^-3
Counts/bin
m=2
m=3
m=4
^{234}U(n,γ)
E_r = 5.16 eV
E_r = 31.13 eV
E_r = 48.56 eV
E_r = 77.38 eV
E_r = 94.29 eV
E_r = 111.06 eV
Av. resonance
E_r = 146.25 eV
E_r = 152.16 eV
Sum energy (MeV)
Gamma energy (MeV)

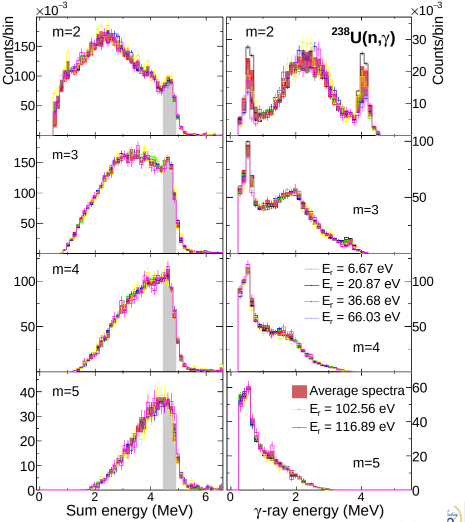
×10^-3
Counts/bin
m=2
m=3
m=4
m=5
^{238}U(n,γ)
E_r = 6.67 eV
E_r = 20.87 eV
E_r = 36.68 eV
E_r = 66.03 eV
Average spectra
E_r = 102.56 eV
E_r = 116.89 eV
Sum energy (MeV)
γ-ray energy (MeV)

Simulations of MSC and sum-energy spectra

Cascades from DICEBOX simulation

$$\Gamma_{i\gamma f} = \sum_{XJ} y^2_{ifXJ}(E_i - E_f)^{2J+1}\frac{f^{(XJ)}(E_i - E_f)}{\rho(E_i, J_i, \pi_i)}$$

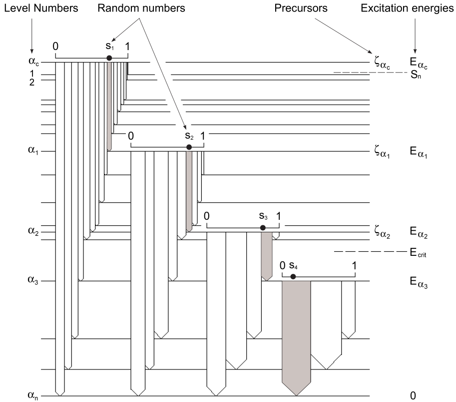

Simulations of MSC and sum-energy spectra

Cascades from DICEBOX simulation

$$\Gamma_{i\gamma f} = \sum_{XJ} y_{ifXJ}^2 (E_i - E_f)^{2J+1} \frac{f^{(XJ)}(E_i - E_f)}{\rho(E_i, J_i, \pi_i)}$$

are fed to GEANT4 detector response of TAC

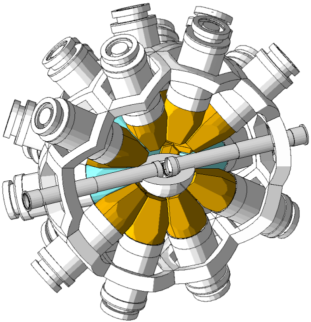

Simulations of MSC and sum-energy spectra

Cascades from DICEBOX simulation

$$\Gamma_{i\gamma f} = \sum_{XJ} y^2_{ifXJ}(E_i - E_f)^{2J+1} \frac{f^{(XJ)}(E_i - E_f)}{\rho(E_i, J_i, \pi_i)}$$

are fed to GEANT4 detector response of TAC

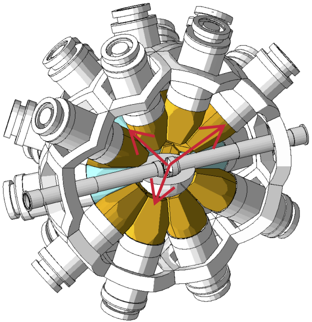

Nuclear levels and their decay/excitation

Lane and Lynn defined the photon strength function $S^{(XL)}$ as rescaled smoothed cross section:

$$S^{(XL)}(E_\gamma) = \frac{1}{(\pi\hbar c)^2}\frac{\overline{\sigma}_\gamma^{(XL)}(E_\gamma)}{(2L+1)E_\gamma^{2L-1}}, \tag{1}$$

or related to the partial radiation width according to Bartholomew:

$$S^{(XL)}(E_\gamma) = \frac{\overline{\Gamma}_{i\gamma f}^{(XL)}(E_\gamma)\rho(E_i,J_i,\pi_i)}{E_\gamma^{2L+1}}, \tag{2}$$

These two definitions are connected by detailed-balance principle:

$$\overline{\Gamma}_{i\gamma f}^{(XL)}(E_\gamma)\rho(E_i,J_i,\pi_i) = \frac{E_\gamma^2}{(\pi\hbar c)^2}\frac{1}{2L+1}\overline{\sigma}_{\gamma,f\to E_i}^{(XL)}(E_\gamma), \tag{3}$$

Giant Electric Dipole Resonance

- measured in (γ,xn) experiments
- from classical electrodynamics – this collective mode in $E1$ PSF should be described by Lorentzian shape
  $S^{E1}_{SLO} = \frac{1}{3(\pi \hbar c)^2} \frac{\sigma_G E_G \Gamma_G^2}{(E_\gamma^2 - E_G^2)^2 + E_\gamma^2 \Gamma_G^2}$
- positions E_G, widths Γ_G and cross sections σ_G obtained from fits of data
- extrapolation below S_n uncertain $\Rightarrow$ phenomenological models: KMF, GLO, EGLO, MGLO, ... and calculations

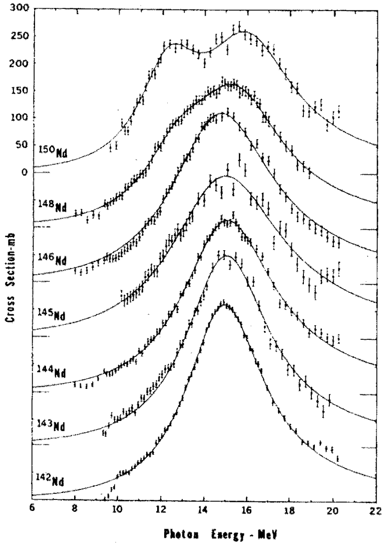

Giant Electric Dipole Resonance

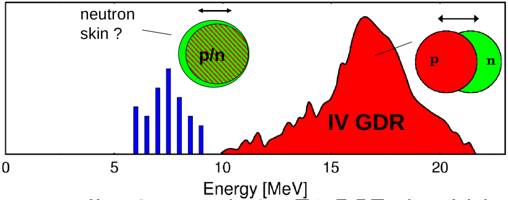

collective mode in $E1$ PSF should be described by Lorentzian shape

$$S^{E1}_{SLO} = \frac{1}{3(\pi \hbar c)^2} \frac{\sigma_G E_G \Gamma_G^2}{(E_\gamma^2 - E_G^2)^2 + E_\gamma^2 \Gamma_G^2}$$

- positions E_G, widths Γ_G and cross sections σ_G obtained from fits of data
- extrapolation below S_n uncertain $\Rightarrow$ phenomenological models: KMF, GLO, EGLO, MGLO, ... and calculations

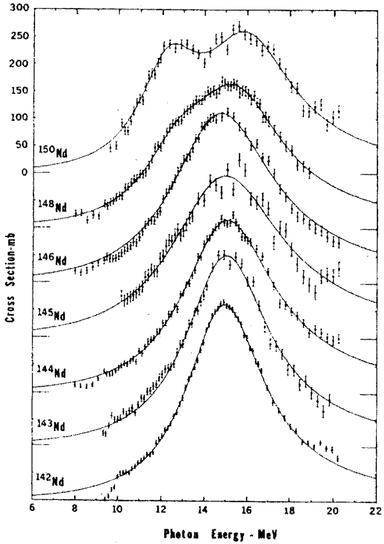

Scissors Mode

- *M*1 collective states in deformed nuclei predicted by theory: Interacting Boson Model, Two-Rotor Model
- experimentally discovered in (e,e') on ^{156}Gd
- measured in nuclear resonance fluorescence scattering (NRF; (γ,γ')) for many rare-earths and later for actinides
- $\Rightarrow$ experimental SM strength dependence on ...
- in decay confirmed from neutron capture & in light ion induced reactions – Oslo method
- the results from different reactions usually agree on the position of SM, but sometimes differ in strength

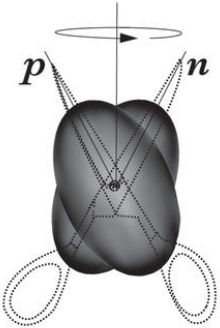

Scissors Mode

- $M1$ collective states in deformed nuclei predicted by theory: Interacting Boson Mode Two-Rotor Model
- experimentally discovered in (e,e') on ^{156}Gd
- measured in nuclear resonance fluorescence scattering (NRF; (γ,γ')) for many rare-earth and later for actinides
- $\Rightarrow$ experimental SM strength dependence on
- in decay confirmed from neutron capture & light ion induced reactions – Oslo method
- the results from different reactions usually agree on the position of SM, but sometimes differ in strength

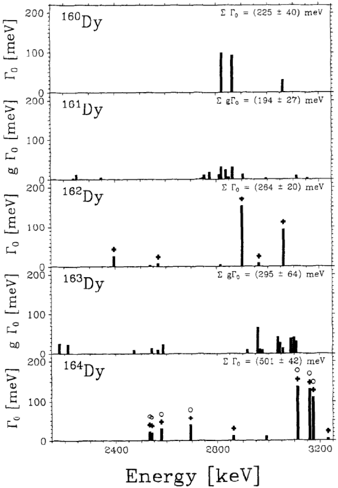

Scissors Mode

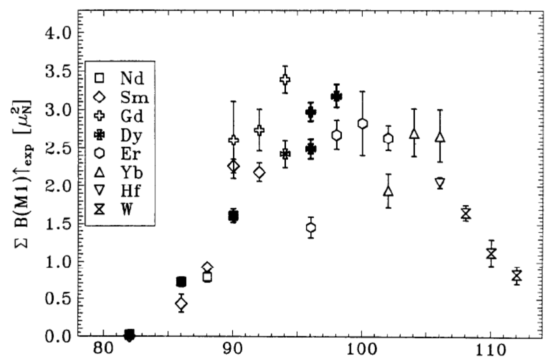

- $M1$ collective states in def
  predicted by theory: Intera
  Two-Rotor Model
- experimentally discovered
- measured in nuclear reson
  scattering (NRF; (γ,γ')) f
  and later for actinides
- $\Rightarrow$ experimental SM strength dependence on ...
- in decay confirmed from neutron capture & in light ion induced reactions – Oslo method
- the results from different reactions usually agree on the position of SM, but sometimes differ in strength

Scissors Mode

- $M1$ collective states predicted by theory: Two-Rotor Model
- experimentally disco
- measured in nuclear scattering (NRF; (γ, and later for actinide
- $\Rightarrow$ experimental SM

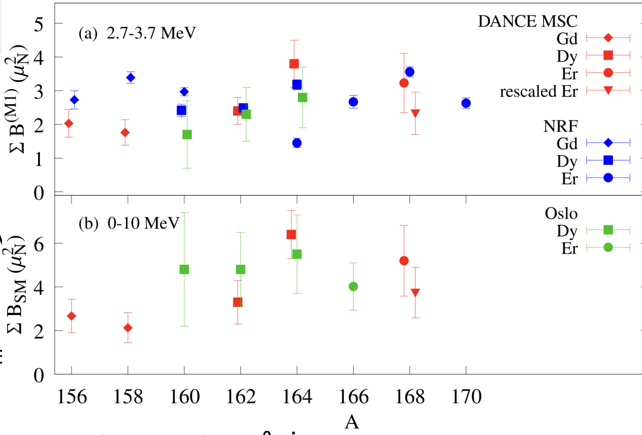

- in decay confirmed from neutron capture & in light ion induced reactions – Oslo method
- the results from different reactions usually agree on the position of SM, but sometimes differ in strength

Model combinations from literature

- from **RIPL-3** database: the analytical **GLO** model for $E1$ PSF and the spin-flip **SF** Lorentzian for $M1$ PSF coupled with the constant-temperature **CT** NLD model,
- the PSFs models proposed in recent **IAEA-19** Coordinated Research Project based on **microscopic** calculations combined with some phenomenological parts used with microscopically based **HFB** plus combinatorial NLD,
- the original model interpretation of the **Oslo** PSF and NLD data: **EGLO** $E1$ model, the **SM** and **SF** $M1$ Lorentzians, and the **CT** NLD,
- **DANCE** model combination: **MGLO** $E1$ model, the **SM** and **SF** $M1$ Lorentzians, and the **CT** NLD

Model combinations from literature

- from **RIPL-3** database: the analytical **GLO** model for $E1$ PSF and the spin-flip **SF** Lorentzian for $M1$ PSF coupled with the constant-temperature **CT** NLD model,
- the PSFs models proposed in recent **IAEA-19** Coordinated Research Project based on **microscopic** calculations combined with some phenomenological parts used with microscopically based **HFB** plus combinatorial NLD,
- the original model interpretation of the **Oslo** PSF and NLD data: **EGLO** $E1$ model, the **SM** and **SF** $M1$ Lorentzians, and the **CT** NLD,
- **DANCE** model combination: **MGLO** $E1$ model, the **SM** and **SF** $M1$ Lorentzians, and the **CT** NLD

Model combinations from literature

- from **RIPL-3** database: the analytical **GLO** model for $E1$ PSF and the spin-flip **SF** Lorentzian for $M1$ PSF coupled with the constant-temperature **CT** NLD model,
- the PSFs models proposed in recent **IAEA-19** Coordinated Research Project based on **microscopic** calculations combined with some phenomenological parts used with microscopically based **HFB** plus combinatorial NLD,
- the original model interpretation of the **Oslo** PSF and NLD data: **EGLO** $E1$ model, the **SM** and **SF** $M1$ Lorentzians, and the **CT** NLD,
- **DANCE** model combination: **MGLO** $E1$ model, the **SM** and **SF** $M1$ Lorentzians, and the **CT** NLD

Model combinations from literature

- from **RIPL-3** database: the analytical **GLO** model for $E1$ PSF and the spin-flip **SF** Lorentzian for $M1$ PSF coupled with the constant-temperature **CT** NLD model,
- the PSFs models proposed in recent **IAEA-19** Coordinated Research Project based on **microscopic** calculations combined with some phenomenological parts used with microscopically based **HFB** plus combinatorial NLD,
- the original model interpretation of the **Oslo** PSF and NLD data: **EGLO** $E1$ model, the **SM** and **SF** $M1$ Lorentzians, and the **CT** NLD,
- **DANCE** model combination: **MGLO** $E1$ model, the **SM** and **SF** $M1$ Lorentzians, and the **CT** NLD

Literature $E1$ PSFs of ^{239}U

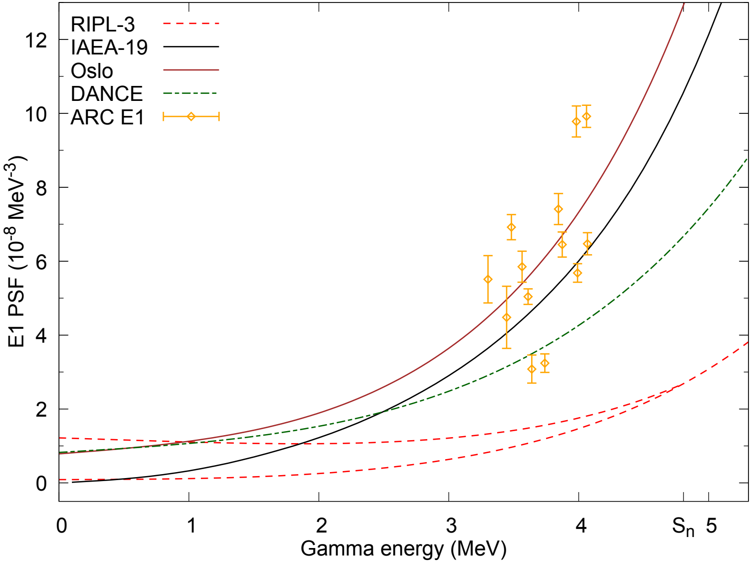

Literature $M1$ PSFs of ^{239}U

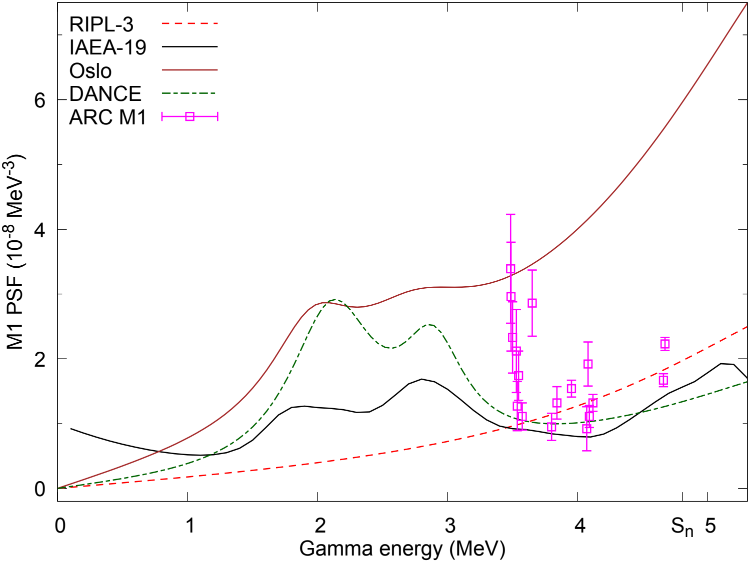

Literature NLD of ^{239}U

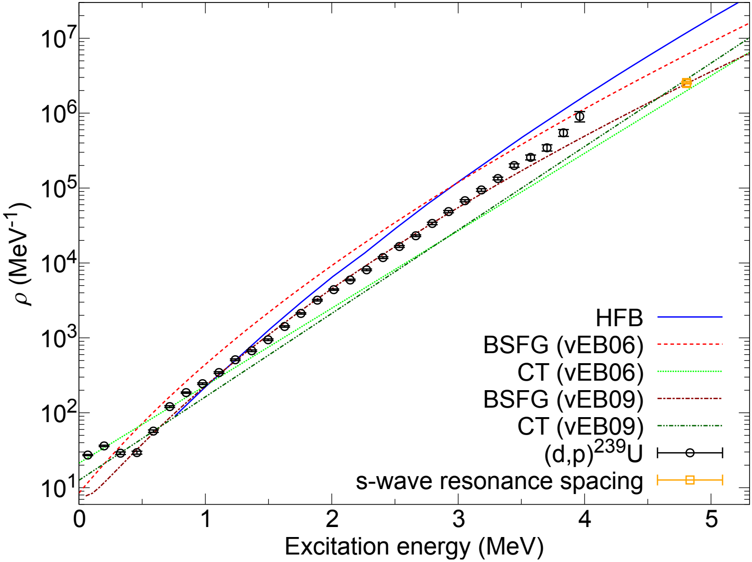

$^{235,239}U$ – RIPL-3 & IAEA-19

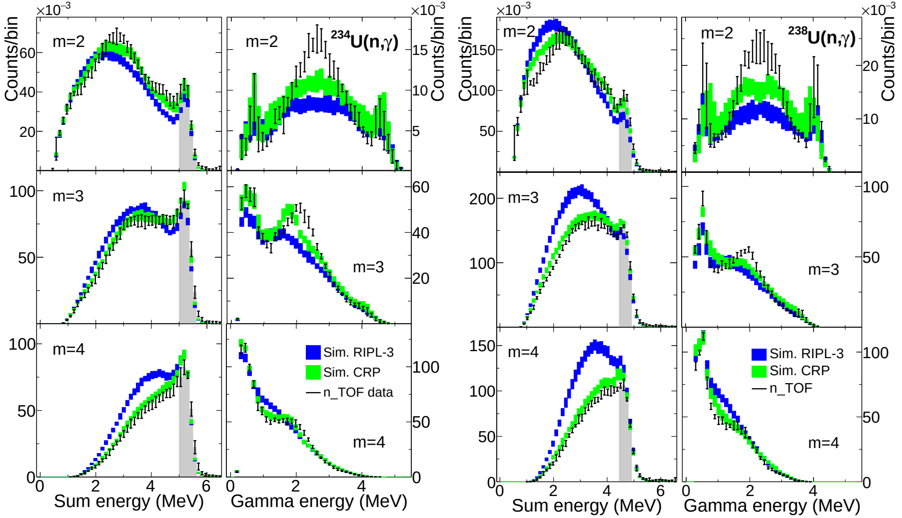

$^{235,239}U$ – Oslo & DANCE

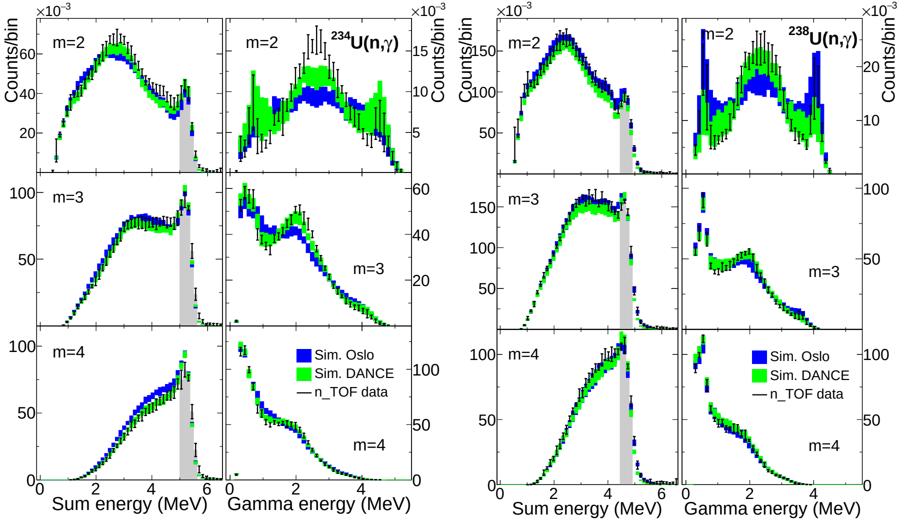

$^{235,239}U$ – adjusted PSFs from n_TOF analysis

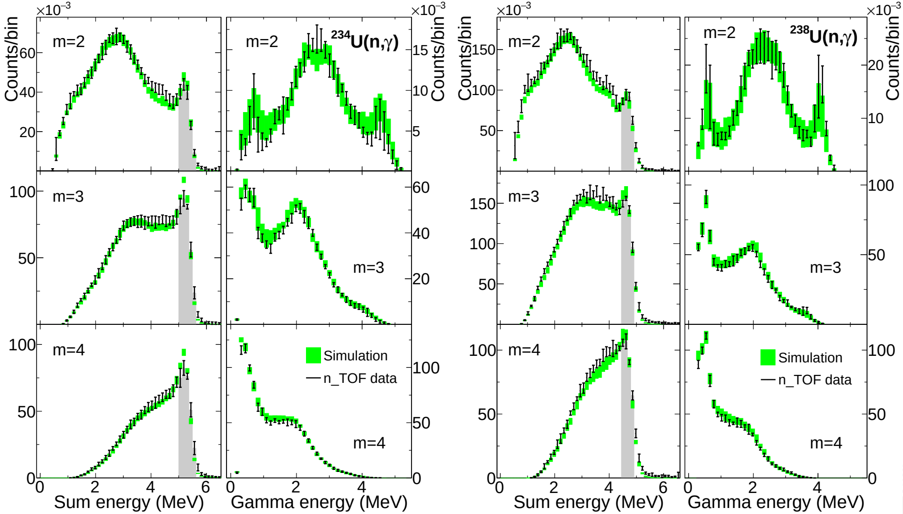

^{239}U – MGLO with $k = 3$ vs $k = 1.8$

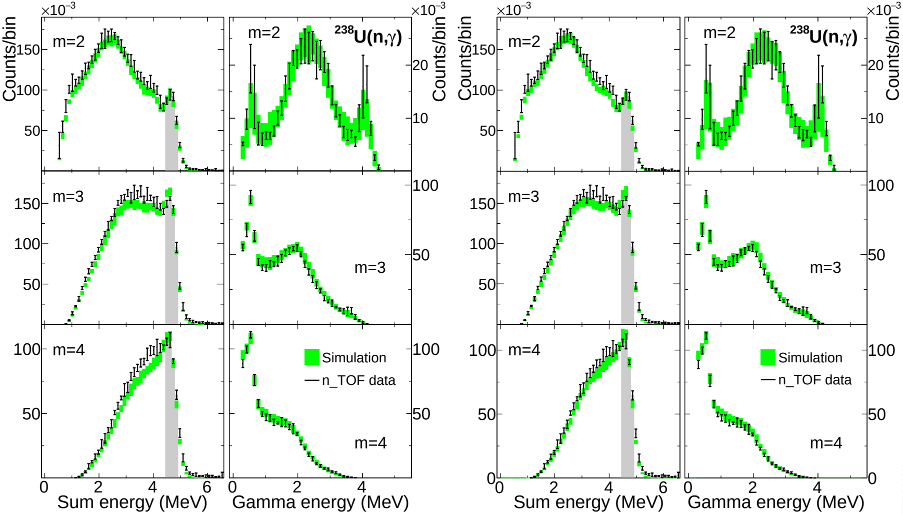

Model combination PSF-LD	Γ_γ (meV) ^{234}U(n,γ)	^{236}U(n,γ)	^{238}U(n,γ)
RIPL-3	16.1(2)	12.9(2)	9.5(2)
IAEA-19	29.4(6)	19.3(5)	13.9(5)
Oslo	19.9(4)	20.4(6)	18.6(8)
DANCE	22.0(5)	17.2(4)	15.9(6)
MGLO(1.8)	**25.4(7)**	20.1(5)	15.9(6)
MGLO(2.5)	30.5(10)	**23.9(7)**	18.8(7)
MGLO(3.0)	39.0(12)	30.9(9)	**24.3(9)**
MGLO$(k, T(E))$	26.7(7)*	24.5(6)†	19.2(7)‡
Mughabghab's atlas 2006	**25.3(10)**	**23.4(8)**	**23.36(31)**
Mughabghab's atlas 2018	36.7(7)	23.4(8)	22.9(4)
JEFF-3.3	26.0	23.0	22.5
ENDF/B-VIII.0	26.0	19.5	22.5

* with $k = 1.8$; † with $k = 2.5$; ‡ with $k = 3.0$

Resulting $E1$ PSF for ^{239}U

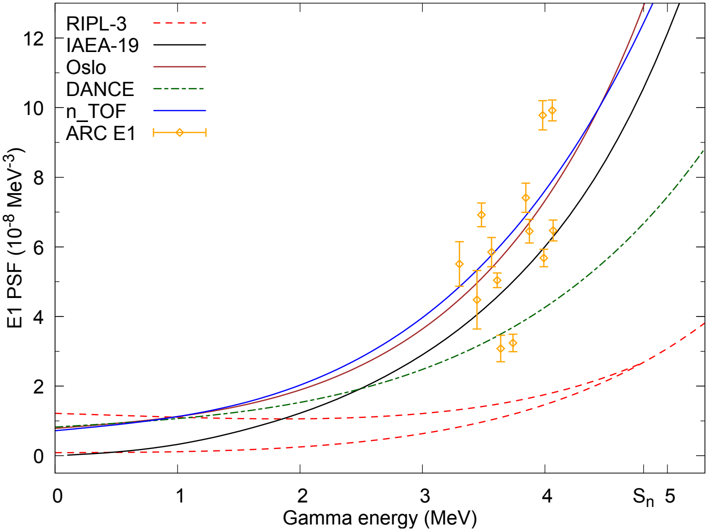

Resulting $M1$ PSF for ^{239}U

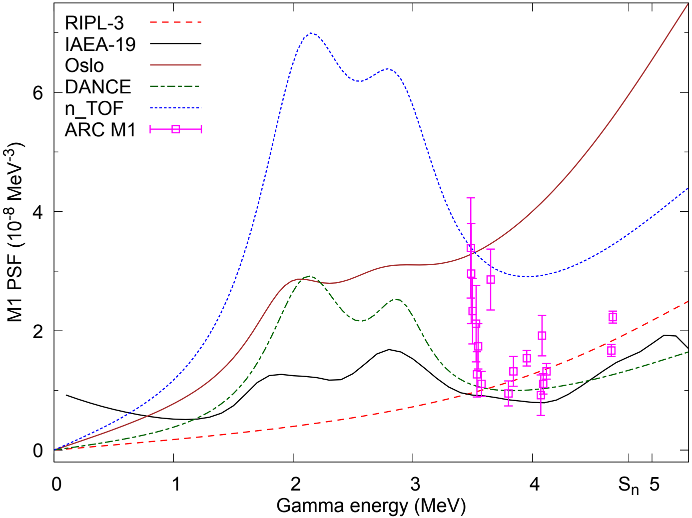

Resulting dipole PSF for ^{239}U

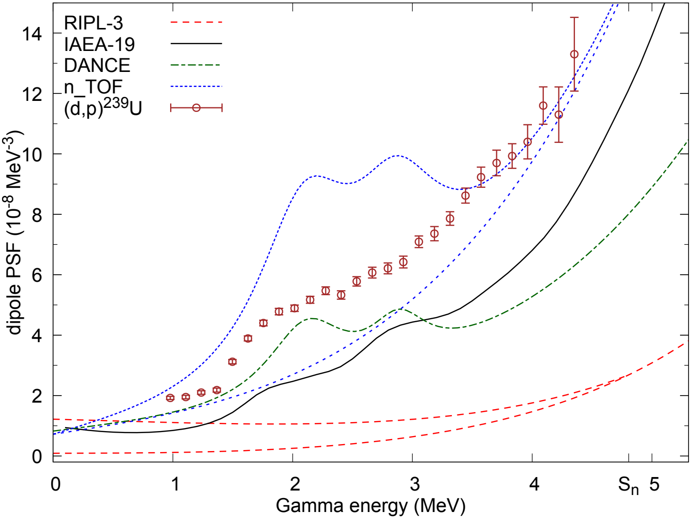

LD and PSFs in odd U's

- sum-energy and MSC spectra of ^{odd}U measured with TAC at n_TOF
- no available model combination is able to describe our data
- we have performed extended search to find a satisfactory reproduction of our experimental spectra
- and we succeeded, see 10.1103/PhysRevC.105.024618 ;)
- CT LD is strongly favored (with unique parameters for each isotope)
- MGLO model is able to describe the $E1$ PSF for energies from 0 to GEDR region
- scissors mode strongly influences decay below S_n, two-resonance form is strongly favored
- taking Γ_γ's into account implies there are no universal PSFs for odd U's, i.e. SM strength increases with mass

LD and PSFs in odd U's

- sum-energy and MSC spectra of $^{\text{odd}}\text{U}$ measured with TAC at n_TOF
- no available model combination is able to describe our data
- we have performed extended search to find a satisfactory reproduction of our experimental spectra
- and we succeeded, see 10.1103/PhysRevC.105.024618 ;)
- CT LD is strongly favored (with unique parameters for each isotope)
- MGLO model is able to describe the $E1$ PSF for energies from 0 to GEDR region
- scissors mode strongly influences decay below S_n, two-resonance form is strongly favored
- taking Γ_γ's into account implies there are no universal PSFs for odd U's, i.e. SM strength increases with mass

LD and PSFs in odd U's

- sum-energy and MSC spectra of $^{\text{odd}}\text{U}$ measured with TAC at n_TOF
- no available model combination is able to describe our data
- we have performed extended search to find a satisfactory reproduction of our experimental spectra
- and we succeeded, see 10.1103/PhysRevC.105.024618 ;)
- CT LD is strongly favored (with unique parameters for each isotope)
- MGLO model is able to describe the $E1$ PSF for energies from 0 to GEDR region
- scissors mode strongly influences decay below S_n, two-resonance form is strongly favored
- taking Γ_γ's into account implies there are no universal PSFs for odd U's, i.e. SM strength increases with mass

LD and PSFs in odd U's

- sum-energy and MSC spectra of $^{\mathrm{odd}}\mathrm{U}$ measured with TAC at n_TOF
- no available model combination is able to describe our data
- we have performed extended search to find a satisfactory reproduction of our experimental spectra
- and we succeeded, see 10.1103/PhysRevC.105.024618 ;)
- CT LD is strongly favored (with unique parameters for each isotope)
- MGLO model is able to describe the $E1$ PSF for energies from 0 to GEDR region
- scissors mode strongly influences decay below S_n, two-resonance form is strongly favored
- taking Γ_γ's into account implies there are no universal PSFs for odd U's, i.e. SM strength increases with mass

LD and PSFs in odd U's

- sum-energy and MSC spectra of $^{\text{odd}}\text{U}$ measured with TAC at n_TOF
- no available model combination is able to describe our data
- we have performed extended search to find a satisfactory reproduction of our experimental spectra
- and we succeeded, see 10.1103/PhysRevC.105.024618 ;)
- CT LD is strongly favored (with unique parameters for each isotope)
- MGLO model is able to describe the $E1$ PSF for energies from 0 to GEDR region
- scissors mode strongly influences decay below S_n, two-resonance form is strongly favored
- taking Γ_γ's into account implies there are no universal PSFs for odd U's, i.e. SM strength increases with mass

LD and PSFs in odd U's

- sum-energy and MSC spectra of $^{\text{odd}}\mathrm{U}$ measured with TAC at n_TOF
- no available model combination is able to describe our data
- we have performed extended search to find a satisfactory reproduction of our experimental spectra
- and we succeeded, see 10.1103/PhysRevC.105.024618 ;)
- CT LD is strongly favored (with unique parameters for each isotope)
- MGLO model is able to describe the $E1$ PSF for energies from 0 to GEDR region
- scissors mode strongly influences decay below S_n, two-resonance form is strongly favored
- taking Γ_γ's into account implies there are no universal PSFs for odd U's, i.e. SM strength increases with mass

LD and PSFs in odd U's

- sum-energy and MSC spectra of $^{\mathrm{odd}}$U measured with TAC at n_TOF
- no available model combination is able to describe our data
- we have performed extended search to find a satisfactory reproduction of our experimental spectra
- and we succeeded, see 10.1103/PhysRevC.105.024618 ;)
- CT LD is strongly favored (with unique parameters for each isotope)
- MGLO model is able to describe the $E1$ PSF for energies from 0 to GEDR region
- scissors mode strongly influences decay below S_n, two-resonance form is strongly favored
- taking Γ_γ's into account implies there are no universal PSFs for odd U's, i.e. SM strength increases with mass

LD and PSFs in odd U's

- sum-energy and MSC spectra of $^{\mathrm{odd}}$U measured with TAC at n_TOF
- no available model combination is able to describe our data
- we have performed extended search to find a satisfactory reproduction of our experimental spectra
- and we succeeded, see 10.1103/PhysRevC.105.024618 ;)
- CT LD is strongly favored (with unique parameters for each isotope)
- MGLO model is able to describe the $E1$ PSF for energies from 0 to GEDR region
- scissors mode strongly influences decay below S_n, two-resonance form is strongly favored
- taking Γ_γ's into account implies there are no universal PSFs for odd U's, i.e. SM strength increases with mass

Thank You for listening!

SM two- or single- resonance? $E1$ Pygmy?

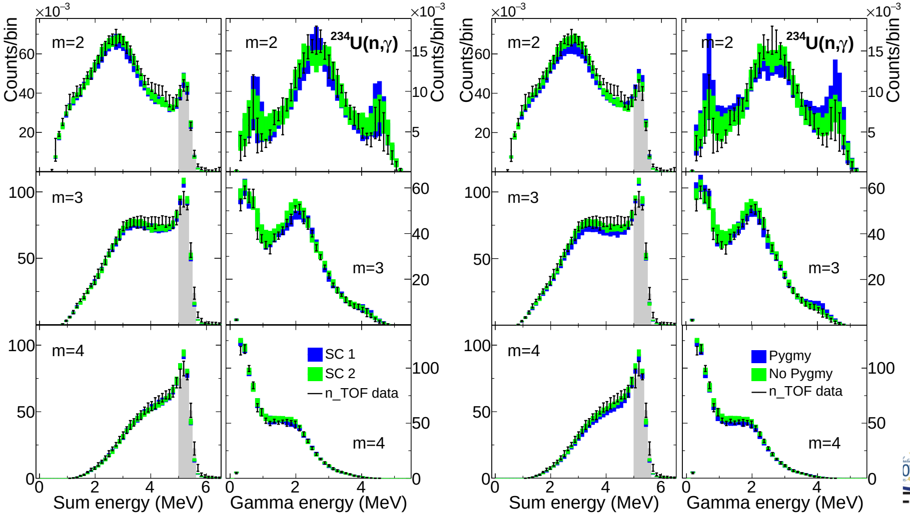

LEE? For moderate one we can not say.

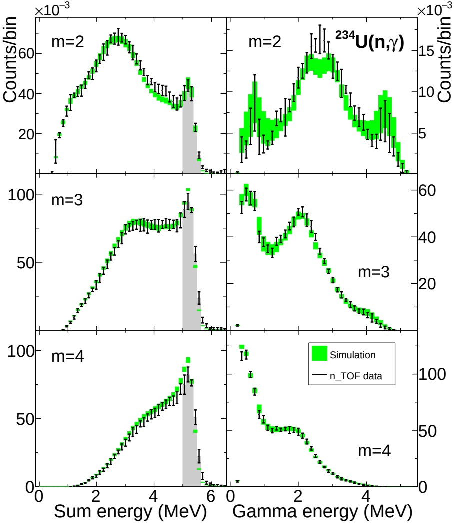

The influence of LEE depends on its shape and magnitude.
In general LEE shifts the multiplicity to higher values, but the footprint in spectra is not so straightforward due to gamma energy threshold.
Note that if LEE is sizable and “squished” to very low energies, the internal conversion will hide its presence in MSC spectra. The question would then be if there are so many electrons flying out?

Footprint of individual SM resonance terms